Chain Mobility in Polymer Systems: On the Borderline between Solid and Melt. 2. Crystal Size Influence in Phase Transition and Sintering of Ultrahigh Molecular Weight Polyethylene via the Mobile Hexagonal Phase

S. Rastogi,* L. Kurelec, and P. J. Lemstra

Eindhoven Polymer Laboratories/The Dutch Polymer Institute, Eindhoven University of Technology, P.O. Box 513, 5600 MB Eindhoven, The Netherlands

Received February 20, 1998; Revised Manuscript Received April 7, 1998

ABSTRACT: Polymorphism is a well-established phenomenon in crystalline materials and is important for pharmaceutical and polymeric materials. In our study concerning the processability of polymers, we came across an unusual observation related to polymorphism induced by pressure. The experimental observation is that polyethylene crystals transform from the stable orthorhombic crystal into a transient hexagonal phase. The occurrence of a transient hexagonal phase is shown to be dependent on the polymer crystal size; smaller crystals transform into the transient hexagonal phase at temperatures and pressures much below the thermodynamic critical point Q_o, which is located at $P = 3.6$ kbar and $T = 230$ °C. The crystal size dependence in the phase transition was investigated by in situ X-ray studies in the unirradiated and irradiated solution-crystallized films. Since the chain mobility is rather high in the hexagonal phase, sintering has been attempted via this transient phase using ultrahigh molecular weight polyethylene (UHMW-PE) as a model system. UHMW-PE is an intractable polymer due to its high molar mass but possesses excellent abrasion resistance properties. For this reason it is used as an inlay in demanding applications such as artificial hip and knee joints. The service life of UHMW-PE in these artificial joints, however, is limited due to the poor processing characteristics notably during sintering, and often a second operation is needed to replace the UHMW-PE interface. Sintering via the transient hexagonal phase could provide a solution for this important problem which concerns an increasing number of people.

1. Introduction

Linear polyethylene (high-density polyethylene) has been studied extensively and could be considered as the paradigm for polymer crystallization studies. The linear, regular polyethylene chains crystallize from solution or from the melt, and at ambient temperature and pressure the chains organize themselves into folded-chain crystals possessing an orthorhombic unit cell. This intriguing phenomenon of chain-folding was found in the mid-1950s, and it is nowadays well documented that, notably upon crystallization from dilute solutions, long polyethylene chains form thin platelet crystals of approximately 10 nm thickness.[1]

It is also possible to obtain crystals in which the molecular chains are packed in a parallel register, without chain-folding. Then, the crystal thickness can range up to several micrometers instead of the conventional few tens of nanometers observed in folded-chain crystals. One method to obtain extended-chain polyethylene crystals is to draw folded-chain crystals in a temperature range close to but below the melting temperature. This process of hot drawing effectively transforms the folded chain crystals into more or less extended-chain structures. At present, technological processes have been developed to produce extended polyethylene structures in the form of fibers based on melt-spinning/drawing[2] and based on solution (gel)-spinning of high molar mass polyethylene, in for example the production of the high-performance fiber Dyneema, possessing a specific Young's (E) modulus exceeding 100 GPa,[3] i.e., higher than that of steel.

* To whom correspondence should be addressed.

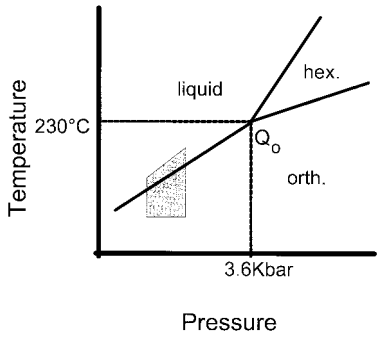

Figure 1. Schematic pressure−temperature phase diagram of polyethylene. Q_o, the equilibrium triple point is the intersection of orthorhombic to hexagonal, hexagonal to liquid, and orthorhombic to liquid transition lines. The shaded region in the figure is the $P-T$ region where experiments have been performed in this work.

Another route to obtain extended-chain polyethylene crystals is to crystallize the polymer at elevated temperatures and pressures. Figure 1 shows the pressure−temperature phase diagram of polyethylene and the occurrence of a triple point Q_o at a pressure of 3.6 kbar and a temperature of 230 °C.[4] Above Q_o, the hexagonal phase is stable between the solid lines. Crystallization at temperatures above the triple point, within the hexagonal phase, leads to the formation of extended-chain crystals. It has been shown experimentally that upon annealing within the hexagonal phase region, initially folded-chain crystals are formed which then thicken continuously into extended-chain structures. This process of lamellar crystal thickening occurs both in the lateral directions and in the chain direction[5] and is attributed to an enhanced chain mobility within the

S0024-9297(98)00261-7 CCC: $15.00
Published on Web 07/10/1998

hexagonal phase.[6,7]

The presence of a hexagonal phase has not been exploited in terms of processing for specific properties. Polyethylene materials possessing extended-chain crystals which are obtained by annealing in the hexagonal phase region are usually brittle materials. This is mainly due to a high crystallinity, the segregation of chains of different molecular weights,[6] and the absence of a physical (entanglement) network.[8] Moreover, the triple point Q_o is beyond the pressure (P) and temperature (T) range which is normally encountered in polymer processing. Consequently, processing and crystallization in the hexagonal phase has remained a rather academic topic up to now.

Recently however, it has been shown using optical microscopy, that a **transient** hexagonal "mobile" phase can appear at pressures and temperatures close to but below the triple point Q_o, i.e., within the thermodynamically stable orthorhombic phase region, upon cooling from the melt.[6,9] In situ X-ray experiments presented in this paper not only will confirm the observation of a transient hexagonal phase, but also will reveal that by controlling the initial morphology during synthesis, this "mobile" phase could be brought down to processable pressures, such as 1 kbar as indicated by the shaded region in Figure 1. The crystal size dependence on the transient nature of the phase has been investigated, both with unirradiated and irradiated (cross-linked) solution-crystallized UHMW-PE.

The observation of this metastable, transient hexagonal phase could be of great significance, mainly due to the enhanced chain mobility in this phase. In view of the fact that the hexagonal phase is a "mobile phase",[4−7,9] processing of polyethylene via this phase could become feasible within an experimentally accessible pressure and temperature range, in particular for ultrahigh molecular weight polyethylenes (UHMW-PEs) which cannot be processed via conventional routes due to the excessive high melt-viscosity.[10]

In this paper we first address the paramount factors which control the occurrence of a metastable hexagonal phase, and second, the results will be used to improve the sintering behavior of UHMW-PE.

2. Experimental Section

2.1. Materials. In view of the complex (sub)structure of UHMW-PE reactor powders, we initially took as a **model** system, solution-crystallized lamellar crystals of UHMW-PE (Hostalen Gur 4130, kindly provided by Hoechst) by dissolving the 1% of polymer by weight at the elevated temperatures, T >125 °C, in xylene. Before dissolution, the UHMW-PE/xylene suspension was degassed and, after complete dissolution, the solution was poured into a tray. A film of approximately 0.4 mm thickness was obtained by slow evaporation of solvent at ambient conditions. When viewed edge-on along the film thickness, small-angle X-ray scattering and transmission electron microscopy showed well-stacked lamellae of a uniform thickness of approximately 12 nm thickness. The transmission electron micrograph in Figure 2 shows the stacked lamellar crystals viewed edge-on. A detailed study on the annealing behavior of these films at the atmospheric pressure has been published elsewhere.[11]

For sintering purposes, a specially synthesized UHMW-PE was made at DSM Research. These low-temperature polymerized, so-called virgin or nascent reactor powders consist of small lamellar crystals with an estimated fold length of 8−10 nm.

The reason for using solution-crystallized UHMW-PE as a model system is that well-defined stacked lamellar crystals are obtained; viz., they are easy to characterize in term of crystal dimensions.[11] In the nascent reactor powders, stacking of lamellar crystals is absent.

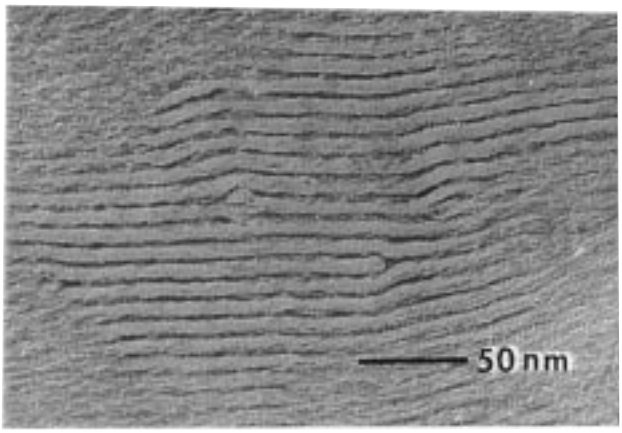

(a)

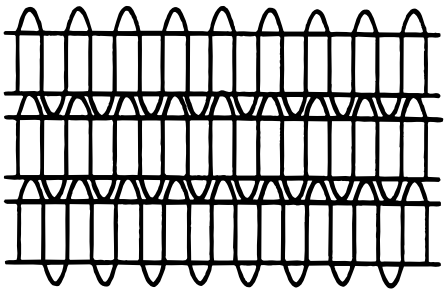

(b)

Figure 2. Transmission electron micrograph of solution-crystallized UHMW-PE. Edge-on view of stacked lamellar crystals of approximately 12 nm thickness can be observed. A schematic drawing is shown in Figure 2b. Molecular chains are perpendicular to the observed edge-on view of the crystals. The micrograph is obtained from a RuO_4-etched thin section of the microtoned sample. The sample was microtoned at liquid nitrogen temperature.

2.2. Instrumentation. The pressure cell used in this study is similar to the one designed by Hikosaka and Seto.[12] The maximum attainable pressure in the present setup is 5 kbar, and the temperature could be varied between room temperature and 300 °C. The sample of 0.4 mm thickness is placed between two diamond windows, each of 1 mm thickness and surrounded by Teflon spacer rings. The use of diamond windows provides the possibility to perform in situ X-ray and optical studies. Hydrostatic pressure is generated by means of two pistons activated by regulated nitrogen gas. The smooth motion of the pistons permitted the maintainance of a constant pressure during any volume change due to phase transformation. Monochromatic X-rays of wavelength 0.968 Å and high flux available on beamline ID11-BL2 at the European Synchrotron Radiation Facility (ESRF), Grenoble, France, was used to overcome the X-ray absorption by diamond windows and to follow the kinetics of phase transformation. Each diffraction pattern was recorded for 30 s on a two-dimensional Princeton CCD detector. Using FIT2D program, kindly provided by Dr. Hammersely of ESRF, 2D X-ray patterns were transformed into one-dimensional patterns by performing an integration along the azimuthal angle.

Some samples were irradiated with a 3 MeV Van de Graaf accelerator at the Interuniversity Reactor Institute, Delft, The Netherlands. The solution-crystallized films were mounted on aluminum plates and placed in a box with a window inert for the electron beam. The box was flushed with nitrogen gas during irradiation to prevent oxidative degradation and the temperature of the samples was maintained at 25 °C. In situ small-angle X-ray scattering (SAXS) experiments on these samples were performed at atmospheric pressure, while heat-

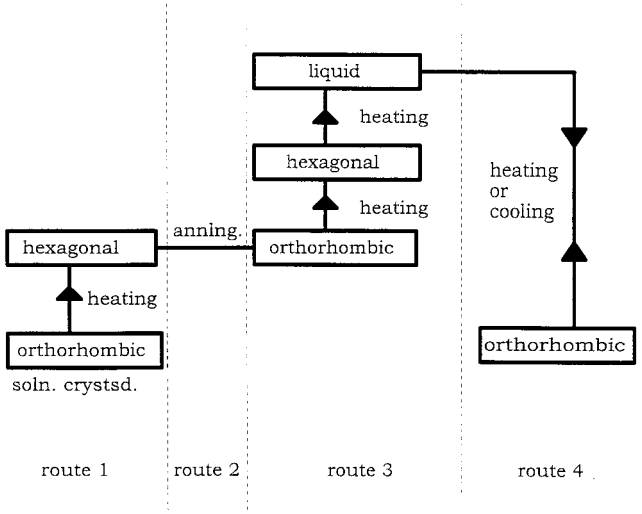

Figure 3. Schematic drawing of the experimental routes adopted in the study of the unirradiated solution and melt crystallized UHMW-PE at the fixed pressure (1.6 kbar), below the equilibrium triple point.

ing, at synchrotron radiation facility available at station 8.2, CLRC, Daresbury, U.K. The X-ray wavelength used for SAXS experiments was 1.54 Å.

3. Results and Discussions

3.1. In Situ X-ray Investigations on Solution-Crystallized UHMW-PE at Elevated Pressures and Temperatures. The following routes were used for the pressure−temperature experiments, shown schematically in Figure 3. In situ X-ray results along the routes have been summarized in Figure 4, and salient features of the results are listed below.

Route 1. Isobaric Heating: Entry of the Hexagonal Phase below the Triple Point. The solution-crystallized UHMW-PE sample was heated at a fixed pressure of 1.6 kbar. The X-ray diffraction pattern at lower temperatures shows the characteristic orthorhombic (110) and (200) reflections (Figure 4a). Upon heating, the (100) reflection of the hexagonal phase though weak appears at approximately 195 °C at $2\theta = 13.42$, next to the (110) reflection of the orthorhombic phase (Figure 4a). The weak intensity of the 100 reflection suggests that only a few but not all crystals have transformed from the orthorhombic to the hexagonal phase. Please note that the pressure of 1.6 kbar is far below the pressure corresponding to the triple point (Figure 1) and that the hexagonal phase is observed within the thermodynamically stable orthorhombic phase.

Route 2. Isothermal and Isobaric Annealing: Isothermal Phase Reversal. Upon annealing at 204 °C at a pressure of 1.6 kbar (route 2 in Figure 3), the (100) reflection of the hexagonal phase disappears again, after approximately 15 min, whereas the orthorhombic reflections gain in intensity (Figure 4b). These results suggest that the crystals which transformed from the orthorhombic to the hexagonal phase transform back into the orthorhombic phase on annealing.

Route 3. Isobaric Heating: Melting via the Hexagonal Phase. During isobaric heating at a rate of 2 °C/min (route 3 in Figure 3), the hexagonal phase reappears, and before final melting at 220 °C, the characteristic (100) reflection of the hexagonal phase gains intensity at the expense of the (110) and (200) reflections of the orthorhombic phase (Figure 4c). Just before complete melting occurs, the only reflection left is 100 of the hexagonal phase.

Route 4. Isobaric Cooling and Heating: Direct Crystallization and Melting via the Orthorhombic Phase. Upon cooling from the melt at the same constant pressure of 1.6 kbar, crystallization occurs directly into the orthorhombic phase, shown in Figure 4d. If the sample is heated once again to the melting temperature, the hexagonal phase is no longer observed (route 4 as shown in Figure 3).

From this set of experiments, we conclude that the melting of the lamellar crystals of approximately 12 nm (initial) thickness proceeds via a **transient** metastable hexagonal phase, much below the triple point and within the thermodynamically stable orthorhombic phase. After complete melting and upon recrystallization from the melt, the appearance of a transient hexagonal phase is not observed again. During heating and annealing of solution-crystallized samples, the thickness of the lamellar crystals increases, especially in the mobile hexagonal phase,[5−7,9] and consequently, the appearance of a transient hexagonal phase could be related with the initial small lamellar thickness. Crystallization from the melt, especially at the elevated pressure, leads to much thicker lamellar crystals compared to solution-crystallized samples, and consequently the shift in the triple-point could be related to the crystal size.

To confirm the influence of the crystal size on the phase transition, we have investigated irradiated solution-crystallized samples. The samples were irradiated with a dose of approximately 2000 kGy. This radiation dose proved to be high enough to prevent lamellar thickening during annealing due to cross-linking at the fold surface. The dose, however, is too low to damage the crystalline core.

3.2. In situ X-ray Investigations on Irradiated Solution-Crystallized UHMW-PE at Atmospheric and Elevated Pressures. Figure 5 shows a set of SAXS patterns, recorded in situ, during heating at atmospheric pressure the irradiated solution-crystallized films. A first-order maximum is observed at $q = 0.052$ Å^{-1} and a second-order maximum at $q = 0.104$ Å^{-1}, satisfying Bragg's condition for a lamellar thickness of 12 nm, at the very early stages of the heating scan, due to the regular periodicity of lamellae in the solution-crystallized sample (Figure 2). Before melting, an increase in the intensity of the first order and a simultaneous disappearance of the second order occur. The increase may be explained because of an increase in the electron density fluctuation between crystalline and amorphous regions due to partial melting of lamellae. The simultaneous disappearance of the second order is due to a loss in the regular periodicity of lamellae in the sample. In contrast, for unirradiated solution-crystallized samples, no appearance of a peak at the lower angles is observed before melting,[11] related to an increase in crystal thickness. This clearly shows that the irradiation dose given to the samples is sufficiently high to cross-link the intercrystalline amorphous zones to prohibit further thickening of lamellae. These irradiated samples were investigated at elevated pressures and temperatures; see below.

Figure 6 shows a set of WAXS experiments performed in situ at a pressure of 1.8 kbar for the irradiated solution-crystallized sample, along the same routes as

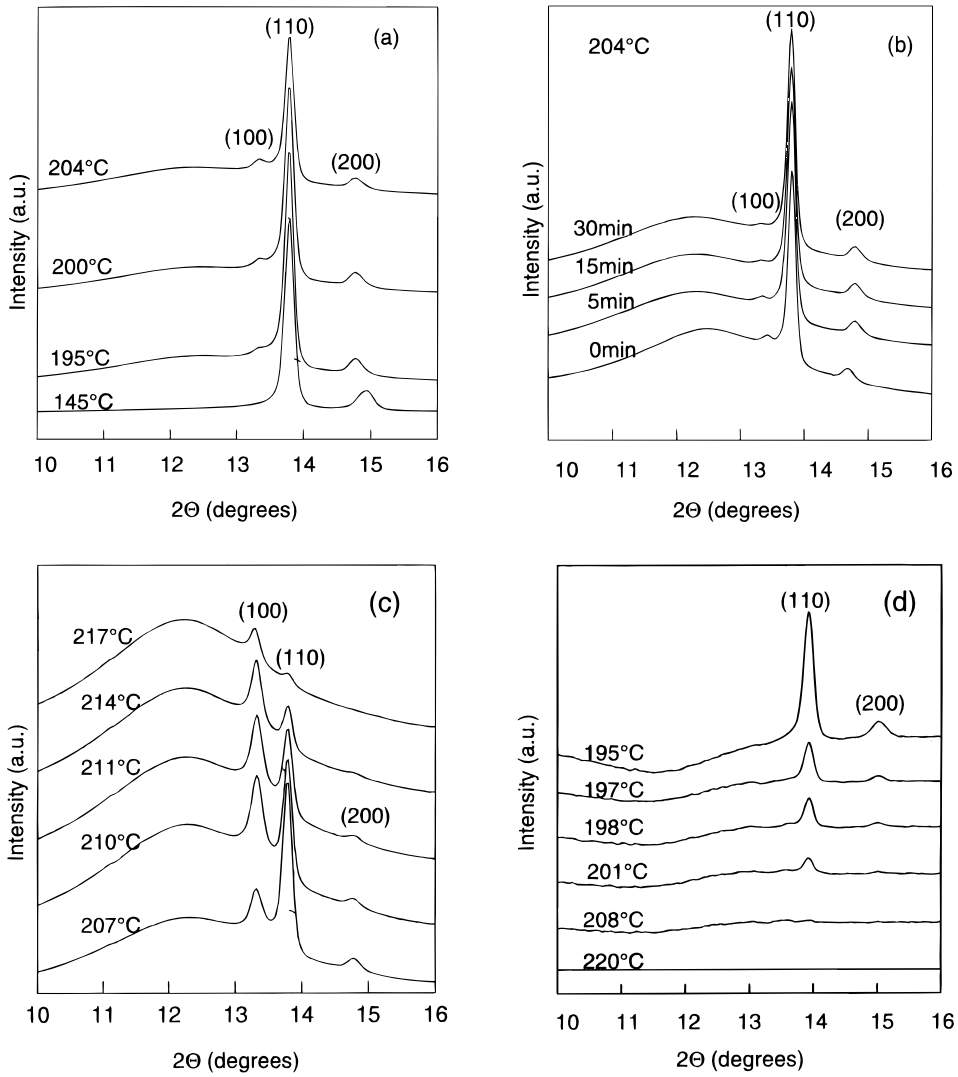

Figure 4. X-ray diffractograms of solution-crystallized UHMW-PE at fixed pressure of 1.6 kbar. Part a shows the entry of the 100 reflection of the hexagonal phase at lower angles, with increasing temperature. The other two reflections are 110 (most intense) and 200 (at higher angle) from the orthorhombic unit cell of polyethylene. Part b shows the disappearance of the 100 reflection of the hexagonal phase during isothermal annealing at 206 °C. During isothermal annealing, while the 100 reflection of hexagonal phase loses intensity, the 110 and 200 reflections of the orthorhombic phase gain intensity. Part c shows the melting of the orthorhombic crystals via the hexagonal phase, similar to the melting behavior anticipated above the triple point Q_o, in the pressure−temperature phase diagram in Figure 1. Part d shows the crystallization via the orthorhombic phase from the melt in the bulk; to observe the very initial stages of crystallization each diffraction pattern is subtracted from the diffuse melt spectrum.

shown schematically in Figure 3 but with remarkably different results, especially along routes 2 and 4. To maintain the thermodynamic parameters similar to the unirradiated solution-crystallized samples, the experiments were performed in the vicinity of the pressure region chosen for the unirradiated samples. The experimental observations made along the routes have been summarized below.

Route 1. Isobaric Heating: Entry of the Hexagonal Phase below the Triple Point. In contrast with unirradiated samples, one of the unusual features in the irradiated samples is that on increasing pressure at room temperature, a few crystals initially in the orthorhombic phase transform into the monoclinic phase, resulting into the appearance of a relatively intense (100) peak at $2\theta = 12.53$.[13] The appearance of the monoclinic phase is related with shear during compression. On increasing the temperature isobarically (1.8 kbar), the monoclinic crystals melt and recrystallize into the orthorhombic phase, evidenced by a total increase in the intensity for the (110) and (200) reflections of the orthorhombic phase at 135 °C (Figure 6a). When the temperature is further increased isobarically, the (100) reflection for the hexagonal phase at $2\theta = 13.42$ appears. Similar to the unirradiated sample, Figure 4, the intensity for the hexagonal (100) reflection increases with temperature. It has to be further noted that, similar to the unirradiated sample, the pressure of 1.8 kbar is far below the triple point (Figure 1); i.e., the hexagonal phase appears in the thermodynamically stable orthorhombic phase.

Route 2. Isothermal and Isobaric Annealing. Upon annealing at 172 °C at a pressure of 1.8 kbar (route 2 in Figure 3), the intensity of the (100) reflection of the hexagonal phase does not change, Figure 6b, in contrast with the unirradiated samples.

Route 3. Isobaric Heating: Melting via the Hexagonal Phase. During isobaric heating at a rate of 2 °C/min (route 3 in Figure 3), the remaining crystals in the orthorhombic phase transform into the hexagonal phase before final melting at 200 °C (Figure 6c).

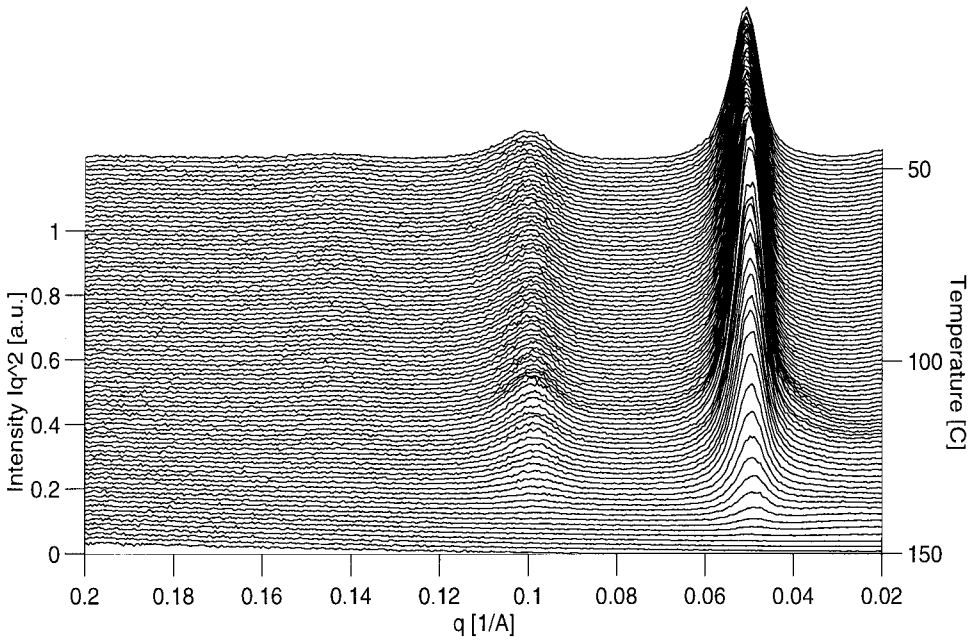

Figure 5. SAXS patterns of the irradiated solution crystallized UHMW-PE film during a heating scan from 50 to 150 °C at 5 °C/min. Each frame was recorded for 12 s, where $q = 2\pi/c$; c is the lamellar thickness.

Route 4. Isobaric Cooling and Heating: Crystallization via the Hexagonal Phase. Upon cooling from the melt, at the same constant pressure of 1.8 kbar, first the appearance of the (100) reflection occurs (Figure 6d). This clearly identifies that even at such low pressures crystallization starts via the hexagonal phase. However, on further cooling, the (110) reflection of the orthorhombic phase becomes more intense. If the sample is heated once again, melting occurs via the hexagonal phase. These observations are rather different to that observed for the unirradiated solution crystallized UHMW-PE samples—where on cooling the sample crystallizes directly in the orthorhombic phase (Figure 4d). From these results it is evident that the triple point for the irradiated samples shifts to much lower pressures. Further investigations performed by us on these samples show that isobaric melting and crystallization via the hexagonal phase, can be achieved even at pressures as low as 1.0 kbar. These experimental findings are in accordance with the high pressure differential thermal studies performed earlier on irradiated polyethylene.[14]

3.3. Salient Features from the Experimental Findings. Before providing a thermodynamic explanation for the observations made on the irradiated and unirradiated samples, it is important to summarize some of the salient features which have emerged from the two sets of experiments (Figures 4 and 6), especially performed along route 2 (Figures 4b and 6b) and route 4 (Figures 4d and 6d). Experiments performed along route 2 clearly show a distinction between the two samples. When the unirradiated sample is annealed isothermally and isobarically, the hexagonal phase transforms back into the orthorhombic phase (Figure 4b) within 30 min, whereas the irradiated crystals, once transformed in the hexagonal phase, stay in the same phase without any transformation even after annealing for more than 150 min (Figure 6b). This distinction in the phase transformation can be explained as a kinetic hindered process in the chain mobility, even in the mobile hexagonal phase, generated by cross-linking the amorphous intercrystalline regions in the irradiated samples—thus maintaining a constant lamellae thickness during annealing. In the unirradiated solution-crystallized samples, on annealing isobarically, isothermal phase reversal occurs, i.e., below the equilibrium triple point Q_o (defined for the extended chain crystals); viz. lamellae thickening during annealing in the mobile hexagonal phase leads to transformation of the initially stable hexagonal phase (for thin crystals) into the thermodynamically stable orthorhombic phase (for thickened crystals).

The crystallization behavior, route 4, for unirradiated and irradiated samples, is also remarkably different. In contrast with the unirradiated sample,[26] the irradiated samples crystallize via the hexagonal phase even below the equilibrium triple point. This may be explained as the crystallization of constrained crystals between a noncrystallizable cross-linked network present in the melt of the irradiated sample. Since the constrained crystals cannot thicken, the lamellae thickness remains constant; thus, the triple point in the $P-T$ phase diagram does not change; see below.

From here it has emerged that the position of the triple point in the P−T phase diagram, Figure 1, is dependent on the lamellae thickness. That is in the unirradiated samples, with lamellae thickening, the triple point for the initially thin crystals (favorable due to kinetic reasons) shifts to the higher pressures and temperatures resulting into the transformation of the initially stable hexagonal phase into orthorhombic phase. In the irradiated samples where lamellar thickening is hindered, the triple point in the $P-T$ phase diagram stays at the same position, thus maintaining stability of the hexagonal phase.

3.4. A Thermodynamic Explanation for the in Situ X-ray Results. Folded-chain lamellar crystals are formed for kinetic reasons,[15] and many studies have been devoted to modeling of the chain folding process in terms of surface nucleation. It is beyond the scope of the present paper to recapitulate the current theories concerning chain folding. It is well accepted that the Gibbs free energy of folded-chain lamellar crystals is higher than for the corresponding extended-chain crys-

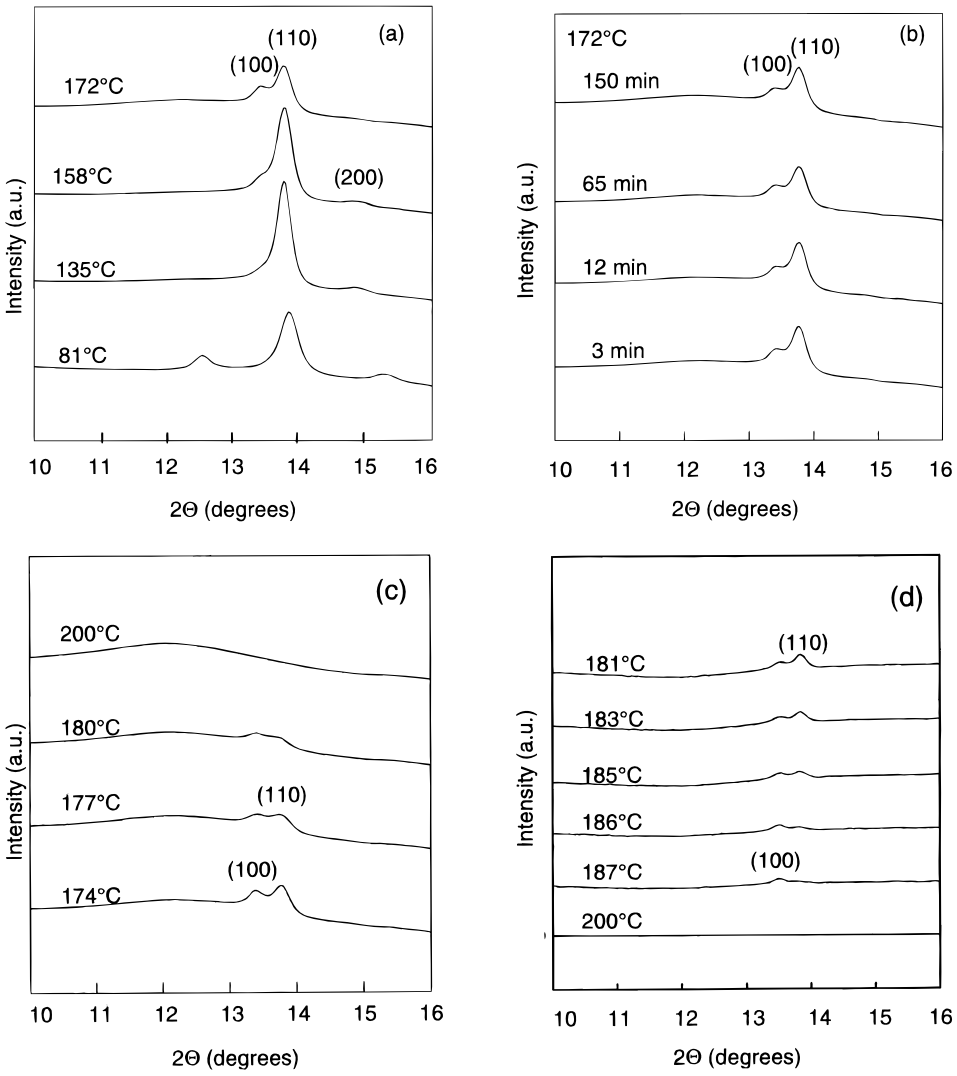

Figure 6. X-ray diffractograms of irradiated solution-crystallized UHMW-PE at fixed pressure of 1.8 kbar. Part a shows the entry of the 100 reflection of the hexagonal phase at lower angles, with increasing temperature. The other two reflections are 110 (most intense) and 200 (at highest angle) from the orthorhombic unit cell of polyethylene. Part b shows the 100 reflection of the hexagonal phase, which stays unaltered during isothermal annealing. Part c shows melting of the orthorhombic crystals via the hexagonal phase, similar to the melting behavior anticipated above the triple point Q_o, in the pressure−temperature phase diagram in Figure 1. Part d shows the crystallization via the orthorhombic phase from the melt. To observe the initial stages of crystallization, each diffraction pattern is subtracted from the melt spectrum.

tals, partly due to the limited crystal size in the chain direction in the order of approximately 10−30 nm. Consequently, the surface energy $2\sigma_e A$, where σ_e is the surface energy of the fold plane and A the corresponding surface, increases the Gibbs free energy. As a consequence, the melting point of folded-chain crystals is lower than for perfectly extended-chain crystals.

The melting point of lamellar crystals with average thickness $\langle c \rangle$ is given by the well-known melting-point depression relationship:[16]

$$T_m = T_m^\circ[1 - 2\sigma_e/\langle c \rangle \Delta H] \qquad (1)$$

As shown in eq 1, the observed melting point (T_m) is dependent on the thickness $\langle c \rangle$; if $\langle c \rangle$ approaches infinity, T_m approaches T_m°, the equilibrium melting temperature.

The ratio $\sigma_e/\Delta H$ for orthorhombic crystals is larger than for hexagonal crystals[17] for the same dimensions of the crystals:

$$(\sigma_e/\Delta H)_{orth} = 3.5(\sigma_e/\Delta H)_{hex}$$

This implies that for the same folded-chain crystal of average lamellar thickness $\langle c \rangle$ the difference ($T_m^\circ - T_m$) is larger in the orthorhombic crystal structure than in the hexagonal crystal structure. Equivalently, the Gibbs free energy for a lamellar crystal with thickness $\langle c \rangle$ is closer to the equilibrium Gibbs free energy G° in the case of a hexagonal crystal structure. On the basis of these experimental facts, the Gibbs free energy diagram in Figure 7, could be constructed to account for the experiments described in Figure 3. *For the sake of simplicity, the Gibbs free energy functions in Figure 7 are drawn as straight lines, which is in fact a simplification to serve the purpose of readability, without any adverse consequences on the interpretation.*

In Figure 7, the Gibbs free energy at pressure P as a function of temperature T is shown for orthorhombic and hexagonal crystals. Below the equilibrium triple point Q_o, the Gibbs free energy of a perfect (extended-chain) orthorhombic crystal, G°_{orth}, is lower than that of a perfect (extended-chain) hexagonal crystal, G°_{hex}. The Gibbs free energy of the folded-chain crystals is higher due to the contribution of the surface free

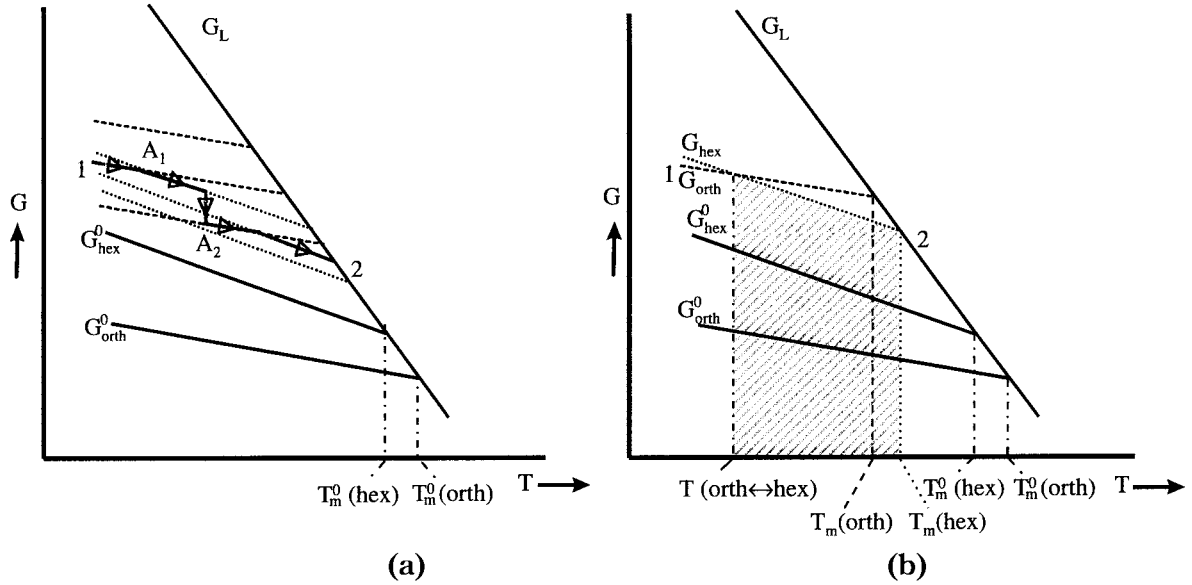

Figure 7. Thermodynamic explanation for the experimental observations made along three different pathways as shown in Figure 3. The bold lines are the equilibrium free energy lines for the orthorhombic $G°_{orth}$, and hexagonal crystal phase $G°_{hex}$. The free energy lines for the orthorhombic folded chain crystals are represented by (- - -), and the hexagonal folded chain crystals are represented by (···). $T_{hex}°$ and $T_{orth}°$ are the equilibrium melting temperatures for the hexagonal and orthorhombic crystals. Parts a and b are for the unirradiated and irradiated samples, respectively. *For the sake of readability, the Gibbs free energy lines are drawn as straight lines instead of curves.*

energies. Assuming for the present discussion that the free energy curves for the folded-chain crystals are parallel with the free energy of the extended-chain crystals and taking into account, as discussed above, that for a given lamellar thickness $\langle c \rangle$ the free energy is closer to equilibrium for hexagonal crystals, the various curves in Figure 7 were drawn schematically as indicated.

3.4.1. The Unirradiated Solution-Crystallized Sample. If an orthorhombic folded-chain crystal with thickness $\langle c \rangle$ is heated from point 1, Figure 7a, at a constant pressure P below Q_o, the corresponding free energy curve crosses the free energy curves of hexagonal folded-chain crystals. At the crossing point A_1, some of the crystals which are thin can transform from an orthorhombic into a hexagonal crystal structure since the decrease in free energy with increasing temperature, (dG/dT), is higher in the case of hexagonal crystals. This situation is encountered during isobaric heating (see Figure 4a). When annealed at temperature T, Figure 4b, the hexagonal crystals thicken in order to decrease the Gibbs free energy toward the equilibrium value, $G°_{hex}$. However, during annealing and thickening at temperature T, once again the Gibbs free energy for the hexagonal and the orthorhombic phase crosses. Further, the driving force $(G°_{hex} - G_{hex})$ becomes smaller and the thickening process slows down and finally is arrested, for example at point A_2. The driving force $(G°_{orth} - G_{orth})$ at temperature T and point A_2 is higher than $(G°_{hex} - G_{hex})$, and consequently, the crystal could transform back into the orthorhombic crystal structure. Upon further heating, Figure 4c, once again, the Gibbs free energy curve corresponding to the orthorhombic crystals crosses many times the Gibbs free energy curves of hexagonal folded-chain crystals. Consequently a transformation from orthorhombic into hexagonal crystals can appear again before the final melting into the liquid phase at point 2.

The authors hasten to add that the above explanation refers only to thermodynamic parameters. The rate of transformation from orthorhombic into hexagonal crystals and vice versa, however, is dependent on kinetic barriers between the two crystal structures. The transformation from the orthorhombic into the hexagonal crystal structure involves nucleation and growth,[18] and consequently, the occurrence of a metastable hexagonal phase and the rate of transformation from orthorhombic into the hexagonal crystal structure and vice versa is system dependent and will depend on parameters like the initial morphology such as crystal thickness, pressure, and temperature. The thickening rate of crystals in the hexagonal phase would be also dependent on the pressure and supercooling;[7,9,18] thus, the resident time of the hexagonal phase would depend on the annealing conditions, like pressure−temperature. In fact, preliminary experiments on other solution-crystallized polyethylene samples, for example a fractionated sample kindly provided by the National Institute of Standard Technology, possessing a M_w of 32 kg·mol^{-1} and a molecular weight distribution M_w/M_n of 1.11, showed that a metastable hexagonal phase appeared at even lower pressures such as 1 kbar.

3.4.2. The Irradiated Solution-Crystallized Sample. A thermodynamic explanation, similar to the unirradiated samples, can also be provided for the irradiated samples. The Gibbs free energy lines drawn in Figure 7b for the irradiated samples are very similar to the unirradiated sample shown in Figure 7a for the fixed pressure P, except G_L moves slightly to higher values for the unirradiated samples. Here we have made a reasonable assumption that during irradiation only the amorphous content in the sample cross links while the crystalline component of the lamellae remains unaffected. Dotted lines in Figure 7b correspond to the Gibbs free energy for the chain folded crystals possessing a 12 nm lamellar thickness. Below the equilibrium triple point, Q_o, for the 12 nm lamellae thickness, the shaded region in the Figure 7b shows the thermodynamic stability regime for the hexagonal phase. Since the lamellae thickness does not change on heating, the

hexagonal phase remains stable even during annealing, as shown experimentally in Figure 6b.[27] On heating, pathway adopted in Figure 7b is the lowest free energy path, i.e., going from the starting point 1 to the melting point 2.

In contrast with the unirradiated samples (Figure 4d), it can be inferred from Figure 6d that, even below 3.6 kbar, crystallization from the melt occurs via the hexagonal phase. This can be explained by constraint in the thickening process during crystallization. Since thickening cannot occur within the constrained crystals (chains between cross-links) as obtained during crystallization from the melt of the irradiated sample, the hexagonal phase will remain stable within the temperature region, shown by shaded region in Figure 7b, at a constant pressure. But if the crystals are not constrained, as is the case in the unirradiated samples, the hexagonal phase present at the initial stages of crystallization will transform into the more stable orthorhombic phase for pressures below the equilibrium triple point.[7,9]

From the present research, it has clearly emerged that the crystal size plays a prominent role in the position of the triple point in the $P-T$ phase diagram of polyethylene. Consequently, in thin crystals an enhanced chain mobility via the hexagonal phase can be achieved at lower pressures, which might be important for sintering; see below.

3.5. Current Problems Associated with Sintering of UHMW-PE Powders. Ultrahigh molecular weight polyethylene, UHMW-PE, is a well-known polyethylene grade possessing excellent mechanical properties such as a high abrasion resistance and excellent wear and friction characteristics compared with any other polymer material. As stated earlier in this paper, due to the high molar mass, UHMW-PE cannot be processed via conventional techniques such as extrusion and injection-moulding. Products based on UHMW-PE are produced by machining semifinished parts such as sheets, rods, and plates, which are obtained by compression-moulding and sintering of UHMW-PE powders. For optimum performance, the UHMW-PE powder particles should be well-fused via sintering/compression-moulding which is a major problem in view of the high viscosity, i.e., the low mobility of the chains to diffuse across the (original) powder interfaces upon sintering in the melt.

In high-performance applications, for example hip and knee joints, improper fusion[19,20] of the submicron size UHMW-PE particles are considered to be one of the main reasons for intracellular and extracellular polyethylene wear debris found upon prosthetic replacement,[21] whereas in the knee-joint prosthesis, grain boundaries present between particles of several tens of micrometer sizes are the weak points to sustain mechanical stresses, leading to delamination.[22] The performance of the prostheses should increase in order to accommodate the active life style and increased life expectancy of the rehabiliated recipient.

Parts a and b of Figure 8 show a closer view of the UHMW-PE hip cups, making use of optical microscopy. Figure 8a shows an optical micrograph of the as-received cup whereas Figure 8b shows the used cup after 7 years. In Figure 8a, grain boundaries related to the original UHMW-PE powder particles can be observed, but they become much more pronounced in the used UHMW-PE cup, Figure 8b. Similar grain

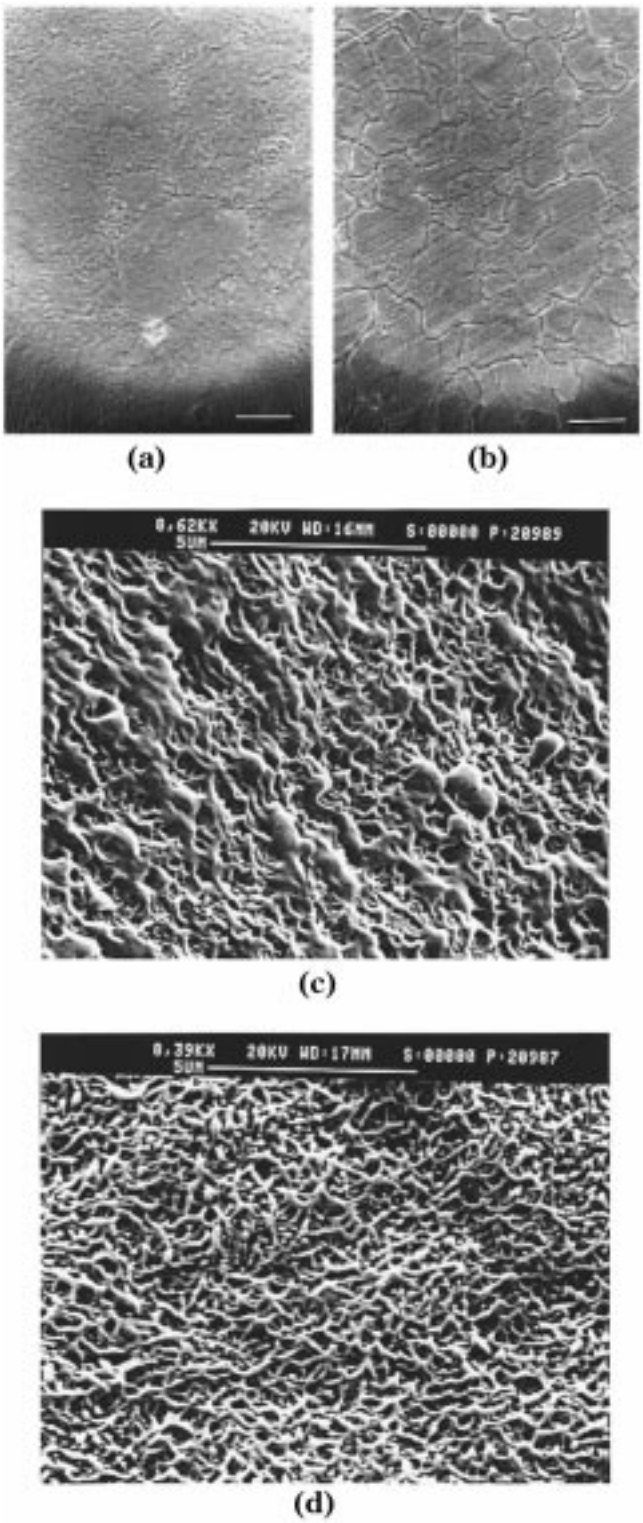

Figure 8. (a and b) Optical micrographs of thin sections of new and used hip cups. Thin sections of approximately 1 μm thickness were prepared by cryosectioning the freeze fractured samples of the hip cups. Part a is the optical micrograph of the as received hip, whereas part b is the optical micrograph of the used hip cup. Scale bar: 100 μm. (c and d) Scanning electron micrographs of freeze-fractured new and used hip cups, respectively. In the electron micrographs interconnected nodular beads may be seen, the holes of submicrometer size are due to removal of the submicrometer sized particles during freeze fracturing. The presence of such nodular substructures is usually seen in the uncompressed UHMW-PE powder [for reference, see Figure 16A-B in ref 14, Mc Kellop et al., and our unpublished work].

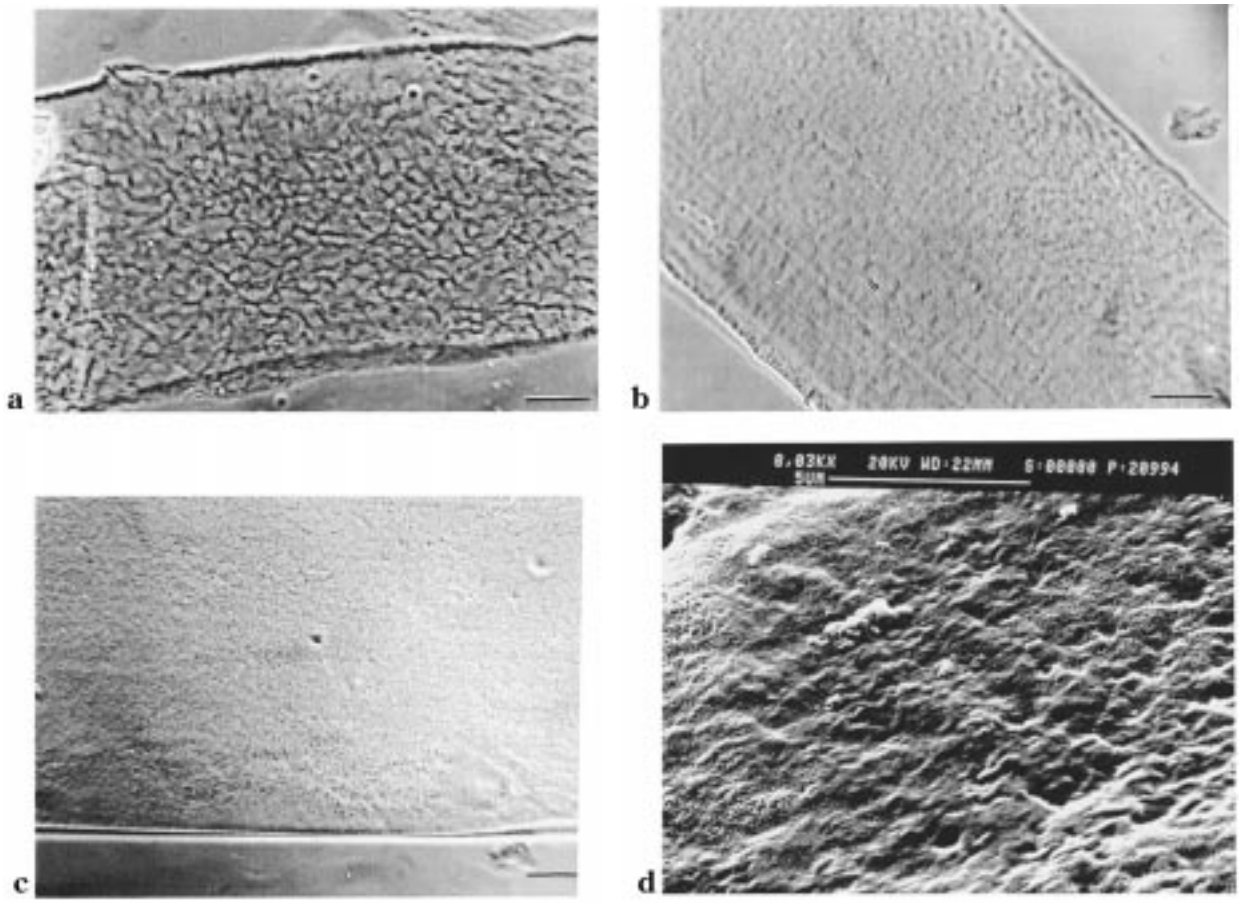

Figure 9. Optical micrographs of thin sections of compression-molded nascent UHMW-PE possessing initially thin crystals of the order of 10 nm lamellae thickness. Part a shows a compression-molded nascent UHMW-PE at 0.8kbar, heated to 205 °C before being cooled to room temperature. Part b is an optical micrograph of the compression-molded nascent UHMW-PE at 1 kbar, heated to 205 °C and then cooled to room temperature. Part c is an optical micrograph of the compression-molded material at 1.2 kbar and 220 °C. Scale bar: μm. Part d is the scanning electron micrograph of the same sample used for part c. Complete absence of the grain boundaries clearly suggest perfect fusion of the particles.

boundaries are observed to be visible in the UHMW-PE inlays used during knee-joint prosthesis. Thenodular substructure present within the powder particles survives during the sintering process as shown in the high magnification scanning electron micrographs, parts c and d of Figure 8, of the new and used hip cups, respectively. Similar nodular substructures have been reported earlier.[23,20] In our opinion, improper fusion, from several tens of micrometers to the submicrometer level, is the main cause for the presence of grain boundaries and at least one of the main reasons for mechanical wear in the prostheses.

3.6. Sintering of Nascent UHMW-PE Powder via the Mobile Hexagonal Phase. In practice, the use of solution-crystallized samples is not very practical in view of large amounts of solvent needed and the cumbersome way of preparation. In this respect, we showed earlier[24] that very small folded-chain crystals can be prepared directly by low-temperature polymerization of ethylene, resulting in nascent reactor powders which, depending on the polymerization conditions, can consist of very tiny lamellar crystals. These crystals in specific nascent reactor powder are highly metastable, and the transition from the orthorhombic into the hexagonal phase can occur at pressures in the proximity of 1 kbar.

Figure 9 shows the effect on the homogeniety of compression-molded nascent UHMW-PE reactor powder via processing involving the "mobile" hexagonal phase. For this study we took a special UHMW-PE reactor powder sample, prepared by DSM, The Netherlands. Figure 9a shows an optical micrograph of the sample compression-molded at 800 bar and 205 °C and subsequently melted and recrystallized from the melt isobarically. Figure 9b shows an optical micrograph of the same material, but now it was compression-molded via the hexagonal phase, as checked by X-ray experiments, at 1.0 kbar and 205 °C and subsequently melted and recrystallized isobarically. This sample, processed via the hexagonal phase, shows a much more homogeneous structure, at least in the central part where no grain boundaries can be observed anymore. The structure becomes completely homogeneous when the pressure is raised above 1.2 kbar, Figure 9c. At the higher magnifications, Figure 9d, the absence of the nodular submicrometer structure is self-evident and a clear distinction in the morphlogy with respect to parts c and d of Figure 8 can be observed.

4. Concluding Remarks

From the in situ X-ray studies performed in this work, using unirradiated and irradiated solution-crystallized UHMW-PE films as a model system, it can be concluded that the location of the triple point in the $P-T$ phase diagram of polyethylene depends on the crystal dimensions, viz., fold length. The crystal dimensions can be controlled by crystallizing from dilute solution or, more practically, at the very initial stage of polymerization,

mainly by monitoring the polymerization temperature. It is shown that the occurrence of a metastable hexagonal phase, well below the triple point, could have important consequences for processing in view of the fact that the hexagonal phase is a so-called "mobile phase" possessing a relatively low viscosity. It is anticipated that improved fusion (at the several micrometer level and consequently at the submicrometer level) will result in much better long-term properties in hip-joint and knee-joint prostheses. To prove this concept, clinical tests which simulate the complex stresses on articles such as artificial hip cups and knee joints are needed and will be performed soon. Further, we have shown another example of isothermal phase reversal, having implications on the phase transformation studies of the condensed matter in general. Similar isothermal phase reversal was observed earlier in *trans*-1,4-polybutadiene at the atmospheric pressure.[25] Making use of the fundamental insight in the chemical and physical aspects, it is shown to be a possible new route to obtain a homogeneous grain free UHMW-PE product—hopefully resolving one of the main causes, due to material characteristics, for the limited lifetime of a prostheses.

Acknowledgment. The authors gratefully acknowledge the experimental facilities available on beamline ID11/BL2 at the European Synchrotron Radiation Facility, Grenoble, France, and station 8.2 at CLRC, Daresbury, U.K. We also wish to thank The Netherlands Research Organization (NWO) for financial support. We also wish to thank Professors M. Hikosaka (Hiroshima University) and A. Keller (Bristol University) for useful discussions.

References and Notes

(1) Keller, A. *Philos. Mag.* **1957**, *2*, 1171.
(2) Capaccio, G.; Crompton, T. A.; Ward, I. M. *J. Polym. Sci., Polym. Phys. Ed.* **1976**, *14*, 1641.
(3) Smith, P.; Lemstra, P. J.; Booij, H. C. *J. Polym. Sci. Polym. Phys. Ed.* **1981**, *19*, 877.
(4) Bassett, D. C.; Khalifa, A.; Turner, B. *Nature (London)* **1972**, *106*; **1972**, *240*, 146.
(5) Wunderlich, B.; Grebowicz, J. *Adv. Polym. Sci.* **1984**, *60/61*, 1. Hikosaka, M. *Polymer* **1987**, *28*, 1257.
(6) Bassett, D.C. *Polymer* **1976**, *17*, 460.
(7) Rastogi, S.; Hikosaka, M.; Kawabata, H.; Keller, A. *Macromolecules* **1991**, *24*, 6384.
(8) Maxwell, A. S.; Unwin, A. P.; Ward, I. M. *Polymer* **1996**, *37*, 3293.
(9) Hikosaka, M.; Rastogi, S.; Keller, A.; Kawabata, H. *J. Macromol. Sci. Phys.* **1992**, *B31*, 87.
(10) Macosko, C. W. *Rheology, Principles, Measurements and Applications*; VCH Publishers Inc.: New York, 1993.
(11) Rastogi, S.; Spoelstra, A. B.; Goossens, J. G. P.; Lemstra, P. J. *Macromolecules* **1997**, *30*, 7880.
(12) Hikosaka, M.; Seto, T. *Jpn. J. Appl. Phys.* **1982**, *21*, L332.
(13) Hay, I. L.; Keller, A. *J. Polym. Sci.* **1970**, *30*, 289.
(14) Vaughen, A. S.; Ungar, G.; Bassett, D. C.; Keller, A. *Polymer* **1985**, *26*, 726. Ungar, G.; Keller, A. *Polymer* **1980**, *21*, 1273.
(15) Armstead, K.; Goldbeck-Wood, G. *Adv. Polym. Sci.* **1995**, *100*, 1.
(16) Hoffman, J. D.; Weeks, I. J. *J. Chem. Phys.* **1965**, *42*, 4301.
(17) Keller, A.; Hikosaka, M.; Rastogi, S.; Toda, A.; Barham, P. J.; Goldbeck-Wood, G. *J. Mater. Sci.* **1994**, *29*, 2579; *Philos. Trans. R. Soc. London* **1994**, *A348*, 3.
(18) Cardew, P. T., Davey, R. J. *Tailoring of Crystal Growth*; Conference of the British Association of Crystal growth; Institute of Chemical Engineers, North Western Branch: Manchester, U.K. (Inst. Civil Eng., 1982). Hikosaka, M.; Amano, K.; Rastogi, S.; Keller, A. *Macromolecules* **1997**, *30*, 2067.
(19) *Proc. Inst. Mech. Eng., Part H: Eng. Med.* **1996**, *210H3*; **1977**, *211H1*.
(20) McKellop, H. A.; Campbell, P.; Park, S. H.; Schmalzried, T. P.; Gregoris, P.; Amstutz, H. C.; Sarmiento, A. *Clin. Orthop. Relat. Res.* **1995**, *311*, 3 and refs 3, 16, 26, and 47 cited therein. Many papers in proceedings mentioned above, like Wang et al., etc. Zachiarades, A. E. Presented at the 17th Annual Meeting of the Society for Biomaterials, Scottsdale, AZ, May 1−5, 1991; p 287.
(21) Schmalzried, T. P.; Jasty, M.; Harris W. H. J. Bone Jt. Surg. **1992**, *74A*, 849. Campbell, P.; Ma, S.; Yeom, B.; McKellop, H.; Schmalzried, P.; Amstutz, H. C. *J. Biomed. Mater. Res.* **1995**, *29*, 127. Hirakawa, K.; Bauer, T. W.; Stulberg, B. N.; Wilde, A. H. *J. Biomed. Mater. Res.* **1996**, *31*, 257 and one of the main conclusions of the proceedings mentioned under ref 13.
(22) Landy, M. M.; Walker, P. S. *J. Arthoplasty* **1988**, *3rd suppl.*, S73. Bartel, D. L.; Bicknell, V. L.; Wright, T. M. *J. Bone Jt. Surg., Am. Vol.* **1986**, *68A*, 1041. Rose, R. M.; Crugnola, A. M.; Ries M. D.; Cimino, W. R.; Paul, I. L.; Radin, E. L. *Clin. Orthop.* **1979**, *145*, 277. Tulp, N. J. A. Wear and Alignment in Total Knee Replacement; an in vivo and laboratory study. Thesis by Katholieke Univeriteit Nijmegen, 1993, Chapter 3 and related papers in the proceedings stated above, especially Figures 3.5 and 3.6 in the thesis.
(23) Wang, A.; Stark, C.; Dumbleton, J. H. *J. Proc. Inst. Mech. Eng., Part H: Eng. Med.* **1996**, *210*, 141.
(24) Engelen, Y. M. T.; Lemstra, P. J. *Polym. Comm.* **1991**, *32*, 343.
(25) Rastogi, S.; Ungar, G. *Macromolecules* **1992**, *25*, 1445.
(26) Our present findings along Route 4 on the unirradiated samples may seem to be in disagreement with the earlier in situ observations made on single crystals, by polarizing optical microscopy.[7,9] The observations then suggested that even in the thermodynamically stable orthorhombic region, close to the triple point (P = 2.8 kbar), crystallization on cooling from the melt proceeds via the hexagonal phase. Such disagreement in experimental results can be a result of a difference in pressures used for optical microscopy (P = 2.8 kbar) and in present X-ray studies (P = 1.6 kbar). Further, the disagreement can be explained as an experimental limitation of the two different techniques used, i.e., optical microscopy and X-ray diffraction. With optical microscopy observations were made on single crystals, whereas in the present X-ray studies data were recorded on bulk samples of 0.4 mm thickness. Since with decreasing pressure and increasing supercooling the residence time for the hexagonal phase decreases exponentially,[7] thus it is practically not feasible to detect a transient phase, nucleating at different time intervals and different positions in the bulk sample even from in situ X-rays.
(27) From Figure 7b, in thicker crystals for the same amount of irradiation doses, the hexagonal phase below Q_o may not be observed. But on increasing the amount of irradiation doses to substantially high values such as 5000 kGy, independent of the initial crystal thickness, the hexagonal phase can be obtained even at the atmopheric pressures.[14] This may be explained from the Gibbs free energy vs Temperature phase diagram, as a shift in the Gibbs free energy, G_{orth}, G_{hex} and G_L, to higher values in the samples (having defected crystals) irradiated to the extreme conditions.

MA980261H